The secret of velvety skin

Article *in* Machine Vision and Applications · September 2003

DOI: 10.1007/s00138-002-0089-7 · Source: DBLP

2 authors:

Jan Koenderink
KU Leuven
629 PUBLICATIONS **25,610** CITATIONS

SEE PROFILE

Sylvia Pont
Delft University of Technology
172 PUBLICATIONS **1,616** CITATIONS

SEE PROFILE

The Secret of Velvety Skin

Jan Koenderink and Sylvia Pont

March 19, 2002

Address of the institution at which the work was done:

Helmholtz Instituut
Universiteit Utrecht
Faculty of Physics and Astronomy
Buys Ballot Laboratory
Princetonplein 5
PO Box 80 000, NL–3508 TA Utrecht, The Netherlands.

Address for correspondence:

Prof. J. J. Koenderink, D.Sc.
Helmholtz Instituut
Universiteit Utrecht
Buys Ballot Laboratory
Princetonplein 5
PO Box 80 000, NL–3508 TA Utrecht, The Netherlands
Telephone: +31 30 2532808
Fax: +31 30 252 2664
e-mail: j.j.koenderink@phys.uu.nl

Abstract

Asperity scattering adds a "surface lobe" to the usual diffuse, backscatter and specular lobes of rough surfaces. Although rarely acknowledged, it is an important effect in many materials that are covered with a thin layer of sparse scatterers such as dust or hairs. In the common case that single scattering predominates, asperity scattering adds important contributions to the structure of the occluding contour and the edge of the body shadow. This is the case because the bidirectional reflectance distribution function (BRDF) is inversely proportional to the cosines of both illumination and viewing angles. The BRDF is generally low (and typically negligible), except when either the illuminating rays or visual directions graze the surface. Because asperity scattering selectively influences the edges in the image of an object, it has a disproportionally (as judged by photometric magnitudes) large effect on (human) visual appreciation. We identify it as a neglected but often decisive visual cue in the rendering of human skin. Its effect is to make smooth cheeks to look "velvety" or "peachy" (the appearances of both velvet and "peachy" skin are dominated by asperity scattering), that is to say, soft. This is a most important aesthetic and emotional factor that is lacking from Lambertian (looks merely dullish, paperlike), "skin–type" BRDF (looks like glossy plastic) or even translucent (looks "hard", vitreous) types of rendering.

Keywords: asperity scattering, skin rendering, velvety look, BRDF, surface modelling.

1 Introduction

For the majority of surfaces from the natural world the BRDF can be sufficiently characterized via just a small number of so called "lobes", namely
— a diffuse lobe
— a backscatter lobe
— an off–specular or specular lobe
— an asperity scattering lobe.
In rare cases (*e.g.*, retroreflective materials, opals, ...) additional lobes may be needed. For most of these lobes there exist familiar phenomenological models, in some cases there even exist (ideal) models of the relevant physics.

The *diffuse lobe* is conventionally described via the "Lambertian assumption" (constant BRDF). There exists no convenient model of the physics that exactly yields a constant BRDF, but the main effect is clearly a thorough scrambling of photon directions due to multiple scattering and/or scattering by randomly oriented microfacets[9].

The *backscatter lobe* is typical for matte surfaces (perhaps roughly Lambertian on a microscale) that are rough on the macroscale (notice that the BRDF *averages* over the macroscale!). Then occlusion and vignetting effects (the "Richardson effect") and the surface attitude effect combine in producing a pronounced backscatter lobe. An exactly solved ideal model is that of a globally planar surface marred by numerous spherical pits[7], an approximate model that captures the same effects is that of random V–shaped grooves on a surface[14].

The (off–)specular lobe occurs in the direction of the classical "mirror" direction. This lobe can be arbitrarily narrow (for a perfect mirror), but is usually broadened due to surface irregularities. It may even be so broad as to go easily unnoticed. For corrugated surfaces the mode of the specular lobe typically shifts a bit (hence is "off–specular"). A well known model is the random mirror model[1]. For deterministic corrugations the specular lobe may split and/or show geometrical structure. (*E.g.*, water waves, human hair[11] , . . .).

The *lobe due to asperity scattering* is much less well documented. It is quite conspicuous for many common materials. The "asperities" can be of various nature, hairtips, dust, "fluff", local high curvature spots or ridges (the term derives from scattering by powdered materials where the "asperities" are sharp edges like on broken glass). In rare cases such as black velvet almost all of the scattering is due to asperity scattering[10]. Asperity scattering is important in many materials though (human hair, skin) and is often very conspicuous near the occluding contour at backlighting conditions.

2 The mechanism of asperity scattering

Asperity scattering is due to scattering by a sparse "cloud cover" of the surface with essentially point scatterers. Since one is only interested in sparse distributions of scatterers one may assume that single scattering predominates. Then parameters of interest are the geometry of the cloud and the nature of the single scatterers.

We assume that the nature of the single scatterers is described via their total scattering cross section σ_t and their phase function $p(\cos\vartheta)$, where ϑ denotes the phase angle, that is the angle subtended by the viewing and illuminating directions[4].

The geometry of the scatterer cloud cover is simple, since we assume a "cover", that is to say, a planar distribution. Thus the geometry is captured through the density of scatterers as a function of "depth" (that is the coordinate in the direction normal to the surface). For the simplest possible

model we assume a uniform distribution of scatterers of thickness Δ. Then the volume density ϱ of the scatterers and the total scattering cross section σ_t determine the mean free path λ of a photon as it travels through the turbid layer. For a thin layer of area A and thickness dz there are $\varrho A\,dz$ scatterers, subtending a total scattering cross section of $\sigma_t \varrho A\,dz$. Thus the probability for a photon of being scattered is $\sigma_t \varrho\,dz$. Then the probability density function $P_s(z)$ for a photon to be scattered after having travelled over a distance z is

$$P_s(z)\,dz = \frac{1}{\lambda}\mathrm{e}^{-\frac{z}{\lambda}}\,dz, \tag{1}$$

with

$$\lambda = \frac{1}{\sigma_t \varrho}. \tag{2}$$

Since we leave the nature of the scatterers completely open, we will assume that the phase function is some arbitrary linear combination of Legendre polynomials[2]

$$p(\cos\vartheta) = \frac{1}{4\pi}(1 + \sum_{n=1}^{\infty} a_n P_n(\cos\vartheta)) \tag{3}$$

Notice that we assume $a_0 = 1$ throughout, and that

$$\int_{(4\pi)} p(\cos\vartheta)\,d\Omega = 1. \tag{4}$$

For $a_1 > 0$, $a_n = 0$ for $n \geq 2$ you have the simplest form of forward scattering, for $a_1 < 0$, $a_n = 0$ for $n \geq 2$ of backward scattering. The peakedness of the scattering indicatrix[2] can be tuned via the higher order coefficients. This enables one to tune the velvety appearance in computer graphics.

In the single scattering approximation a photon enters the layer from a direction $\mathbf{u}$ (say) and exits the layer (at another location) in a solid angle $d\Omega$ centered at the direction $\mathbf{v}$ say, due to a single scattering event within the layer. For the moment we fix the depth at which the scattering occurs, this evidently fixes the complete path. We first find the probability for such an event and consequently integrate it over the depth of the layer.

Let the scattering occur after the photon has traversed a distance in the interval $(s, s+ds)$ within the layer. (See figure 1.) The probability of such an event is the probability of the scattering to occur having travelled a length $(s, s+ds)$ through the layer, times the value of the phase function of argument $-\mathbf{u}\cdot\mathbf{v}$, times the probability of escape from the layer. The escape probability is the probability of not being scattered in the path after the scattering event.

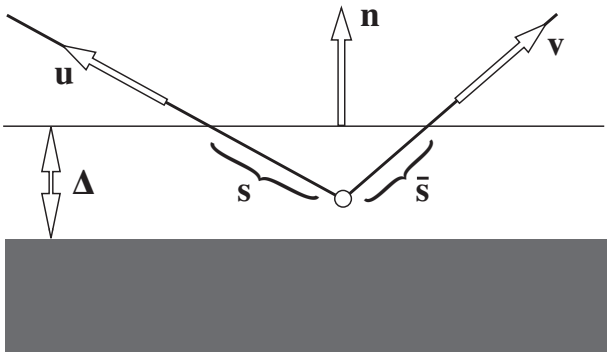

Figure 1: *The basic geometry of asperity scattering. The planparallel layer of thickness* Δ *on a black substrate with outward surface normal* $\mathbf{n}$ *is irradiated from a direction* $\mathbf{u}$ *and viewed from a direction* $\mathbf{v}$*. The pathlength from entrance to the first scattering event is* s*, after scattering the photon has to travel a distance* $\overline{s}$ *before exit. From the geometry one has the basic relation* $s\mathbf{u}\cdot\mathbf{n} = \overline{s}\mathbf{v}\cdot\mathbf{n}$.

The escape probability P_{esc} for a pathlength $\overline{s}$ is

$$P_{esc}(\overline{s}) = \int_{\overline{s}}^{\infty} P_s(\xi)\, d\xi = \mathrm{e}^{-\frac{\overline{s}}{\lambda}} \tag{5}$$

Let the surface normal be $\mathbf{n}$. From the geometry (see figure 1) we have that

$$\overline{s} = \frac{\mathbf{u}\cdot\mathbf{n}}{\mathbf{v}\cdot\mathbf{n}} s. \tag{6}$$

Thus you have for the probability $P(\mathbf{u},\mathbf{v},s)\, ds\, d\Omega$ of scattering of a photon incident from the direction $\mathbf{u}$ into a solid angle $d\Omega$ centered on the exit direction $\mathbf{v}$ at a depth s in a layer of thickness ds:

$$\begin{aligned} P(\mathbf{u},\mathbf{v},s)\, ds\, d\Omega &= P_s(s) p(-\mathbf{u}\cdot\mathbf{v}) P_{esc}(s\tfrac{\mathbf{u}\cdot\mathbf{n}}{\mathbf{v}\cdot\mathbf{n}})\, ds\, d\Omega \\ &= \tfrac{p(-\mathbf{u}\cdot\mathbf{v})}{\lambda} \mathbf{e}^{-\frac{s}{\lambda}\frac{(\mathbf{u}+\mathbf{v})\cdot\mathbf{n}}{\mathbf{v}\cdot\mathbf{n}}}\, ds\, d\Omega \end{aligned} \tag{7}$$

Hence the probability of a ray entering from a direction $\mathbf{u}$ (say) and exiting in a solid angle $d\Omega$ centered at the direction $\mathbf{v}$ via scattering anywhere in the layer is

$$\begin{aligned} P_{scat}(\mathbf{u},\mathbf{v})\, d\Omega &= \textstyle\int_0^{\frac{\Delta}{\mathbf{u}\cdot\mathbf{n}}} P(\mathbf{u},\mathbf{v},s)\, ds\, d\Omega \\ &= p(-\mathbf{u}\cdot\mathbf{v}) \tfrac{\mathbf{v}\cdot\mathbf{n}}{(\mathbf{u}+\mathbf{v})\cdot\mathbf{n}} (1 - \mathrm{e}^{-\frac{\Delta}{\lambda}\frac{(\mathbf{u}+\mathbf{v})\cdot\mathbf{n}}{(\mathbf{u}\cdot\mathbf{n})\,(\mathbf{v}\cdot\mathbf{n})}})\, d\Omega. \end{aligned} \tag{8}$$

This is the required probability.

In many cases we are mainly interested in the bidirectional reflectance distribution function (BRDF) of the layer. It can be derived simply from the probability determined by equation 8. Consider a large area A and uniformly spread N rays over the area. Then the irradiance is N/A rays per unit area. There are $NP_{scat}(\mathbf{u},\mathbf{v})\,d\Omega$ rays in the scattered beam. The étendue of the scattered beam is $A(\mathbf{v}\cdot\mathbf{n})\,d\Omega$, thus the radiance of the scattered beam is $NP_{scat}(\mathbf{u},\mathbf{v})/(A\mathbf{v}\cdot\mathbf{n})$ rays per unit area per unit solid angle. The BRDF is defined as the radiance of the exit beam divided by the irradiance caused by the entrance beam, thus we have

$$f(\mathbf{u},\mathbf{v}) = p(-\mathbf{u}\cdot\mathbf{v})\frac{(1-\mathrm{e}^{-\frac{\Delta}{\lambda}\frac{(\mathbf{u}+\mathbf{v})\cdot\mathbf{n}}{(\mathbf{u}\cdot\mathbf{n})\,(\mathbf{v}\cdot\mathbf{n})}})}{(\mathbf{u}+\mathbf{v})\cdot\mathbf{n}}. \tag{9}$$

Notice that $f(\mathbf{u},\mathbf{v}) = f(\mathbf{v},\mathbf{u})$, thus Helmholtz reciprocity pertains (as expected).

For an optically thin layer we have (expanding the exponential to first order)

$$f(\mathbf{u},\mathbf{v}) \approx \frac{p(-\mathbf{u}\cdot\mathbf{v})(\Delta/\lambda)}{(\mathbf{u}\cdot\mathbf{n})\,(\mathbf{v}\cdot\mathbf{n})} \qquad \Delta << \lambda, \tag{10}$$

This is indeed the desired approximation. In case of a thick layer one needs to take multiple scattering events into account, something we ruled out by assumption. In the simple case of isotropic scatterers we obtain simply

$$f(\mathbf{u},\mathbf{v}) \approx \frac{\text{constant}}{\cos\vartheta_i\cos\vartheta_e} \qquad (\frac{\Delta}{\lambda} << 1 \quad \text{and} \quad p(\cos\vartheta) = \frac{1}{4\pi}), \tag{11}$$

with the constant equal to $f(\mathbf{n},\mathbf{n}) = \Delta/4\pi\lambda$, that is to say the BRDF value for normal incidence and viewing. We set $\cos\vartheta_i = \mathbf{u}\cdot\mathbf{n}$, $\cos\vartheta_e = \mathbf{v}\cdot\mathbf{n}$, thus ϑ_i denotes the angle of incidence, ϑ_e the viewing angle, both taken with respect to the outward surface normal. This expression is perhaps most useful since it enables simple intuitive reasoning about the effects of asperity scattering. The constant $f(\mathbf{n},\mathbf{n})$ can simply be taken as an empirical quantity that needs to be estimated from a single observation.

Notice that the approximation used here implies $\Delta << \lambda$, thus *very low density* materials. Thus the albedo due to asperity scattering should be low. In typical cases the total albedo will be much higher due to other forms of scattering of course. Higher values due to asperity scattering would necessarily imply *multiple* scattering, which again implies that the usual "law of darkening" will replace the typical asperity scattering effects[2].

Notice that expression 11 explodes as either the viewing or illumination direction grazes the surface (thus either $\vartheta_i \approx \pi/2$ or $\vartheta_e \approx \pi/2$). In such

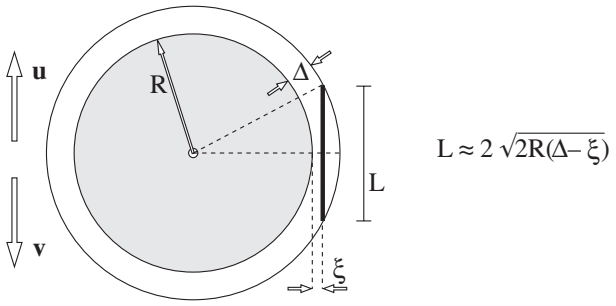

Figure 2: *The rim geometry. The thick line is a generic column of turbid layer aligned along both the viewing direction and the direction of incidence. Thus the column is seen edge–on and is near both the occluding contour and the body shadow boundary. The bulk of the object appears dark against the light, the column is part of the bright halo. The length L depends on R, Δ and ξ, the radiance is simply proportional with it.*

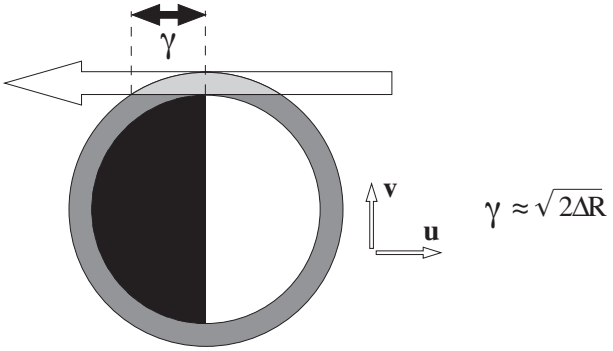

Figure 3: *The geometry near the terminator of the body shadow. The luminous rim bleeds a distance γ into the body shadow area. The width of this rim (γ) depends both on the thickness of the scattering layer Δ and on the radius of curvature of the surface R.*

a case the approximation breaks down. For a flat layer multiple scattering would take over as the pathlength within the scattering layer grows without bounds. Thus we assume that the pathlength in the medium does not exceed λ, which implies that the approximation of expression 11 does not apply when either ϑ_i or ϑ_e approaches $\pi/2$. In the more typical case of *curved* surfaces the pathlength is limited to (approximately) $2\sqrt{2\Delta R}$, where R denotes the radius of curvature of the section perpendicular to the contour. (See figures 2 and 3.) Since the domain of validity of expression 11 excludes only very narrow regions it will usually suffice to simply clip the BRDF. With this simple rule expression 11 can be used for graphical rendering (see 5).

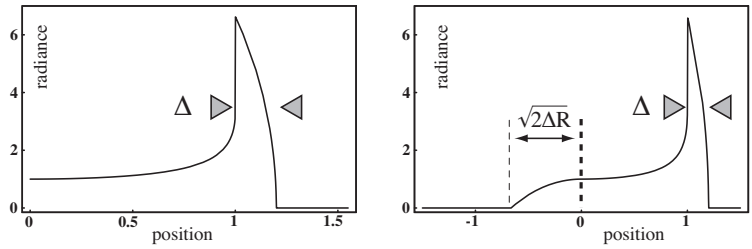

Figure 4: *Effects of asperity scattering for a black sphere of unit radius surrounded with a scattering layer of width* $\Delta = 0.2$. *We assume* $\Delta << \lambda$. *The graphs show the scattered radiance (in arbitrary units) as a function of position in the image (*± 1 *the edges,* 0 *the center of the sphere). On the left the case of illumination from the viewing direction. (The radiance for normal illumination and normal viewing has been arbitrarily set to unity, only the right part of the sphere (occluding boundary at position* $+1$*) has been plotted.) Notice the pronounced bright halo, it is identical to the halo seen against the light. On the right the case of illumination from the side (*90° *phase angle). The edge of the shadow boundary has been indicated (at position* 0*). Notice that the radiance received from the surface extends to regions well within the area of the body shadow. Only one contour has a bright halo in this case.*

Since the scattering takes place within the volume of the layer, the exit ray need not arise from the same nominal position on the surface as the entrance ray. For a cylinder of diameter d the "displacement" can be as much as (approximately) $\sqrt{2d\Delta}$ (see figures 2 and 3), far exceeding the thickness of the scattering layer. This effect is most seen pronouncedly at the edge of the body shadow and in the case of back lighting (figure 4). In the latter case one sees a bright halo of width Δ at the contour. The halo appears even when the source is "behind the horizon" (thus $\vartheta_i > \pi/2$, the utility of the BRDF description itself breaks down here); this is the "twilight" phenomenon that appears in the theories of the optics of planetary atmospheres[15].

The radiance profiles in figure 4 were computed directly from the geometry as the BRDF approximation doesn't allow for extrapolation beyond the occluding contour or the edge of the body shadow. Since the radiance of the scattered beam is directly proportional with the depth of the irradiated column, such calculations are immediate and simple. This method may well be the preferred one (instead of expression 11) in computer graphics rendering.

Since the scattering is thus not completely localized, asperity scattering has the effect of "blurring", much like in the case of translucent layers[6]. Moreover, the very concept of BRDF becomes somewhat problematic, except

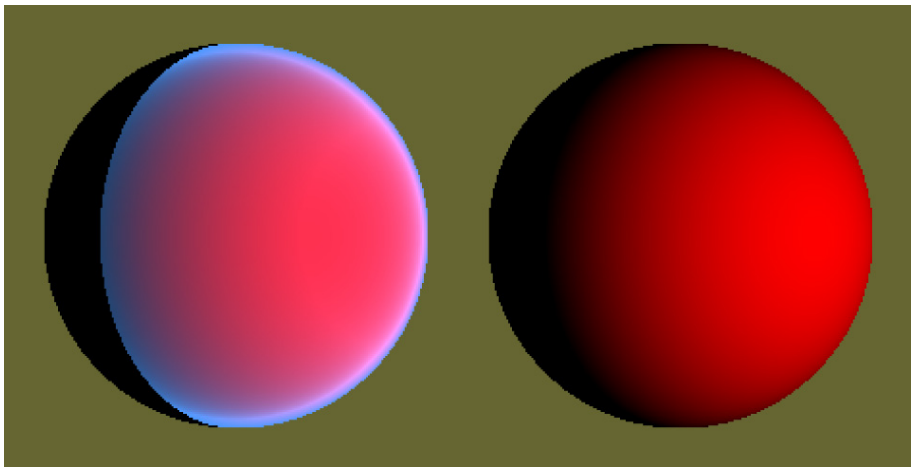

Figure 5: *On the left a rendering of a Lambertian (red) sphere overlaid with a layer of asperities scattering in the blue, on the right a rendering without the contribution due to asperity scattering. A uniform phase function was assumed. Notice that the effects of asperity scattering are especially apparent near the contour and the attached shadow boundary. In this rendering the simple BRDF approximation was used, no attempt was made to take the finite thickness of the layer into account. Whereas the approximation is a crude one, the typical effects of asperity scattering are readily apparent.*

in a spatial average sense. These effects may have a decisive influence on visual appearance (see below), though the quantitative effects are small.

3 Some empirical examples

A prototypical example of asperity scattering is offered by black velvet[10]: Almost *all* of the radiation scattered by this material is due to asperity scattering (see figure 6).

We selected a piece of black velvet for the demonstration and measured the BRDF for viewing directions in the plane of incidence. The velvet was wrapped around a cylinder of 50 mm diameter. The cylinder was mounted in a large room with black walls in order to minimize possible effects of stray radiation. The radiant source and the detector are mounted on stands that may be rotated about the center of the sample. The total size of the setup is several meters, thus allowing much larger samples than is typical for commercially available gonioreflectometers.

The cylinder was irradiated by a collimated beam (angular spread less

Figure 6: *A monochrome photograph of a draped black velvet cloth (left) and a color photograph of a draped yellow velvet cloth (right). In both cases the illumination is frontal, with a collimated beam. Notice that the black velvet looks dark except for places where the visual or light rays graze the surface. In the yellow cloth the same effect can be seen in the color (the asperity scattering is whitish as compared to the body color of the cloth) but is much less apparent due to the lowered contrast.*

than two degrees, uniformity within the beam's cross section better than five percent) derived from a high pressure xenon arc source. The cylinder was imaged by a Leaf camera which uses a linear CCD array to scan the focal plane (24x36mm) of a Nikon mount lens. Dark signal was monitored and subtracted. Each image yields a sequence of 1200 stripes of pixels, each stripe ca. 100 pixels high in the direction of the cylinder axis. We averaged over the stripes and thus obtained a sequence of about 1200 radiance samples for fixed phase angle per image (see figure 7). We varied the phase angle between 10° and 160°, in increments of about 20°.

The sequences were interpolated via a series of Chebyshev polynomials, in this manner we normalized the observations on a uniform rectangular grid in configuration space. Since we limited the observations to the plane of incidence, configuration space can be parameterized by two signed angles, the irradiation angle (henceforth denoted φ) and the viewing angle (henceforth denoted ϑ). As reference direction (zero angles) we used the outward surface normal. Helmholtz reciprocity was enforced by symmetrizing the BRDF $f(\varphi, \vartheta) = f(\vartheta, \varphi)$. Linear interpolation on the uniform rectangular grid reproduces the raw observations very closely, easily within the noise level.

The "noise level" is not set by photon noise, but by the deterministic

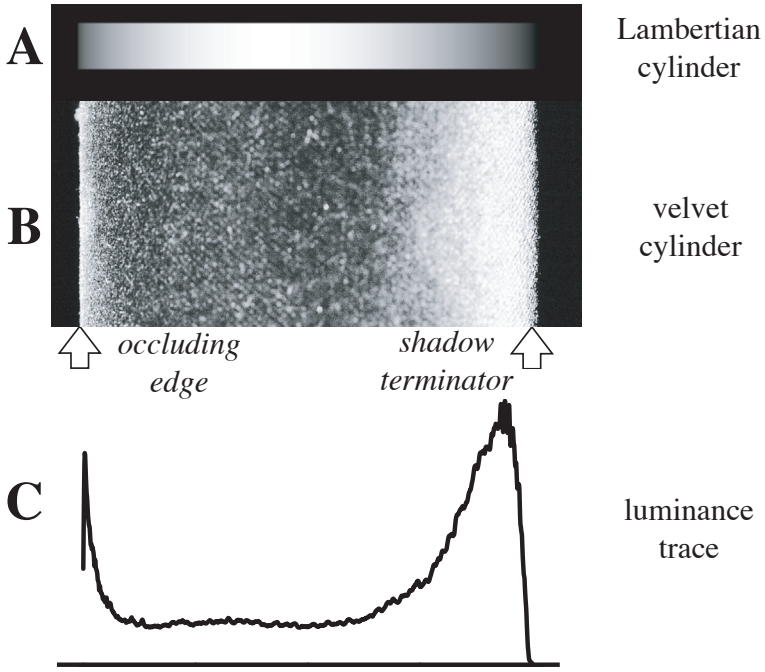

Figure 7: *A picture of the black velvet cylinder (B) for a phase angle of* 10°. *(The image intensity histogram has been skewed in order to obtain a reasonable picture, remember that the velvet is deep black!) The contour of the cylinder ("occluding edge" arrow) and the edge of the shadow boundary ("shadow terminator arrow") have been marked, thus only part of the cylinder is depicted (the remainder being in shadow). Notice the structure of the weave (giving rise to "noise" in the BRDF) and the roughness of both the contour and the shadow edge. The strip at the top (A) depicts the appearance of a Lambertian cylinder. Notice that the velvet is lightest where the Lambertian surface is darkest and* vice versa*; asperity scattering is as non–Lambertian as one gets! On the bottom (C) we show a trace (averaged over the height) of the pixel intensities. Notice the strong scattering at places of grazing viewing (contour at left) or illumination (shadow edge at right).*

structure (the weave and the disarray of the fibers) of the cloth (figure 7). Effects of this structure are clearly visible in the raw data and still somewhat evident in the interpolated BRDF.

Since Helmholtz reciprocity was enforced, the scattering in the specular direction is symmetric ($f(\mu, -\mu) = f(-\mu, \mu)$). One might expect the scattering in the backscatter direction to be symmetric too ($f(\mu, \mu) = f(-\mu, -\mu)$). Although this is not the automatic result of Helmholtz reciprocity, it would

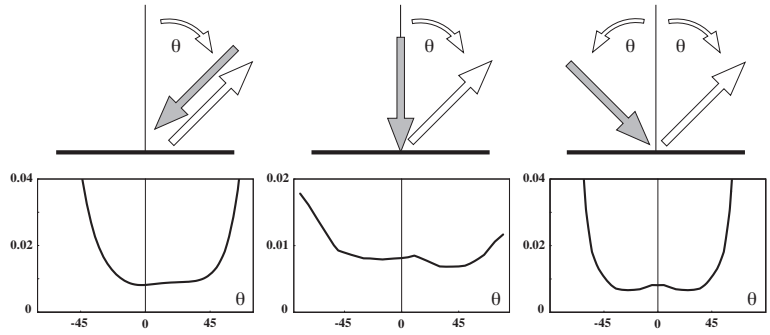

Figure 8: *The BRDF (values plotted on the vertical axis) in the plane of incidence for black velvet. The direction of incidence is indicated with the grey arrows, the viewing direction with the white arrows. The horizontal axis is the viewing angle. As the viewing angle varies the angle of incidence is adjusted to implement pure backscattering (left), normal incidence (center) and specular reflection (right). In the latter case one has bilateral symmetry due to Helmholtz reciprocity. The lack of true bilateral symmetry is evident in the other cases. The basic feature of asperity scattering, that is inverse proportionality with the cosines of illumination and viewing directions is evident.*

be the expected result if the surface were structured isotropically. Our data clearly reject this hypothesis for the present sample though. (See figure 8.) The backscatter characteristic is rather asymmetric. We ascribe this effect to the attitude of the hairs. Although the velvet indeed consists of many tiny hairs that stand "on end", these hairs are actually somewhat (10–20 degrees) slanted with respect to the surface normal. This is typical for velvet and accounts for the obvious visual effects when you slightly stroke velvet, thus pushing its hairs into a preferred direction.

Except for the effect of hair slant, the BRDF measured for the velvet closely follows the predictions of the asperity scattering model. (A slight modification of the phase function allows for the effect of hair slant too.) The parameter Δ/λ turns out to have a value of about 0.1, thus the thin layer (single scattering) approximation is corroborated in retrospect. In figure 9 we present the scattering diagram for the sample. Notice that both backward and forward scattering occur and that the radiance of the scattered beam only assumes appreciable values for viewing directions that almost graze the surface.

The asperity scattering lobe is clearly a "surface lobe" in that the radiance of the scattered beam is highest when the surface is either viewed or irradiated

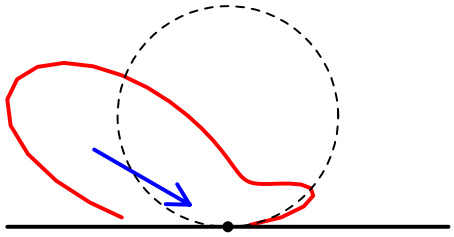

Figure 9: *Scattering diagram for black velvet. In this polar diagram a Lambertian surface would appear as the dashed circle, shown here for easy reference. The angle of incidence is marked with an arrow. Notice the absence of bilateral symmetry due to the fact that the velvet's hairs don't truly "stand on end".*

from a direction almost grazing the surface, and even more so when both irradiating and viewing directions are close to grazing. Although the BRDF of the black velvet is very low for normal irradiation and normal viewing (two orders of magnitude lower than for a white Lambertian surface), at grazing angles the BRDF may approach (or even exceed) the value for a white Lambertian surface. This is the reason for the characteristic appearance of black velvet cloth. The overall impression is that of a black substance, whereas the occluding edges of folds and the edges of body shadow boundaries stand out as light by contrast, the former appearing as sharp contrast edges, the latter as fairly diffuse ones. This is indeed exactly how black velvet garments were painted by the 17^{th}c. Dutch painters. The body of the garment is blocked in black, the edges are superimposed in gray paint, the sharpness of the edges being modulated appropriately. "Shading" in the conventional sense is not applied at all.

We also did measurements on a ripe (reddish–purplish hue) peach. In this case the effects of asperity scattering are largely lost in the (much larger) effects of diffuse and specular scattering. Yet the peach looks very conspicuously different from a nectarine of about the same shape, size and color (see figure 10). Whereas the nectarine looks smooth and glossy, and because of its slight translucency slightly vitreous, the peach looks "soft". This is due to a thin layer of sparse, fibrous material in air that envelopes the surface. Although rather open, thus transparent, this nexus of fibrous material contributes to asperity scattering. Whereas—in frontal, collimated illumination—the lightest part of the nectarine is a specular highlight (broadened because of the irregular surface microstructure, thus contributing to the "glossy" look) and the darkest parts are near its occluding boundary, the lightest parts of the peach occur near the occluding boundary. The light

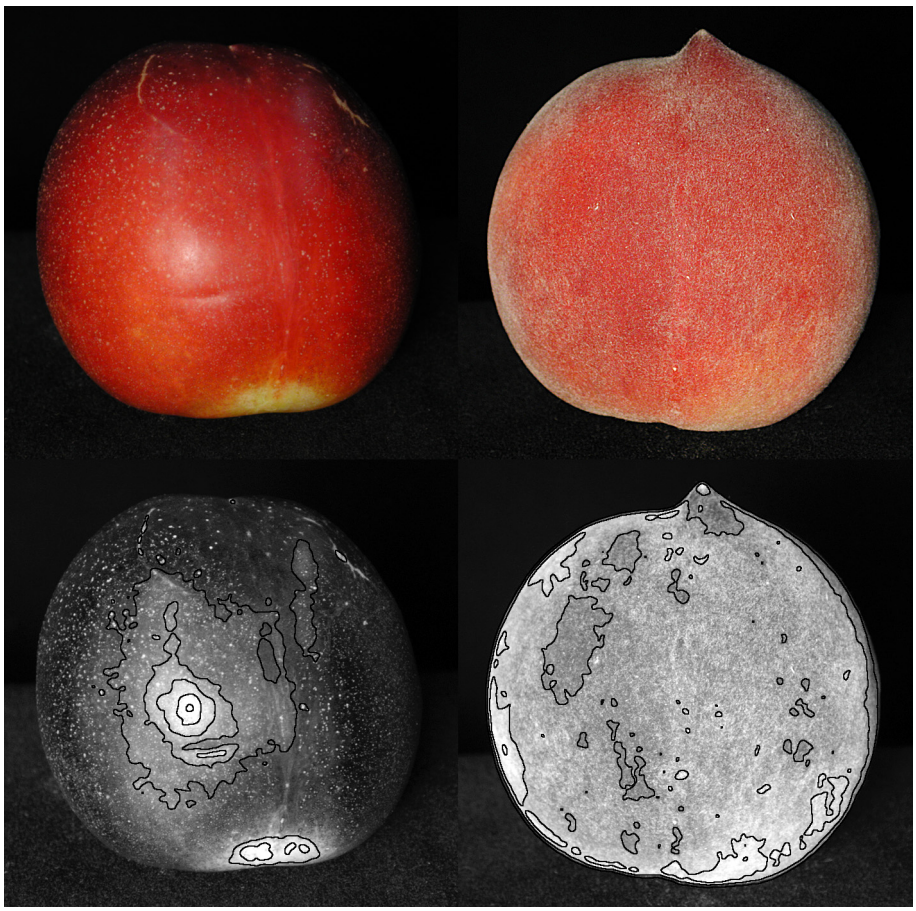

Figure 10: *A nectarine and a peach are both roughly spherical solids of similar color. One is "bald", the other covered with downy hairs. The difference in appearance is mainly due to the presence or absence of asperity scattering and specular gloss in the case of the nectarine. This is clearly apparent from the pattern of isophotes. Compared with the nectarine the peach concentrates lightness near the contour and the shadow edge.*

scattered through asperity scattering has the color of the illuminant, whereas the light scattered from the peach's skin proper is reddish due to selective absorption. As a result the peach appears "soft", "velvety" or (more proper) "peachy" to the eye. The visual difference between the two fruits is very striking and clearly one looks "hard", the other "soft".

We used the same method, exploiting the closely spherical shape of the fruit by treating a surface strip centered on the horizontal equator as an approximate cylindrical surface. We find that the effect of asperity scattering is minor in comparison to the diffuse (or very broad specular) lobe, as indeed

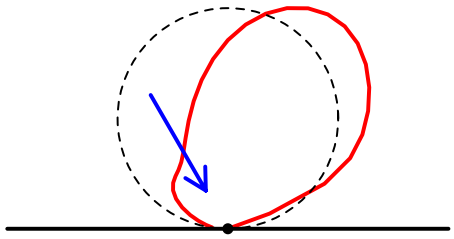

Figure 11: *Scattering diagram for a ripe peach (see also the legend of figure 10). Different from the velvet, the peach has a fairly light surface which is slightly glossy, overlaid with a hairy "atmosphere" that is responsible for the asperity scattering. Although the effect of asperity scattering is quantitatively a minor one, it dominates the visual impression.*

was to be expected. It is just about visible in the scattering diagram shown in figure 11. Yet this somewhat minor photometrical effect apparently has major consequences for visual appearances.

4 Visual appearance and asperity scattering

A great many materials display a variety of asperity scattering. In cases where the asperities can easily be resolved this effect tends to be visually obvious. Examples include hairy surfaces of plants, animals and humans (figures 10 and 12 through 15) which are indeed the rule rather than the exception.

In certain cases the asperities are clearly resolved and also lead to *texture*. The nature of the texture depends critically upon the illumination and viewing angles and thus cannot easily be faked through texture mapping. In cases where the asperities are not easily, or not at all, resolved, the fact that the asperity scattering lobe still modulates the BRDF is easily missed. There exist many such cases, for instance peaches (asperities barely visible) or the skin of young women (asperities hardly perceptible at all without close scrutiny). (Figures 10 through 15.) Yet the effect of the asperity scattering is visually obvious in both examples because the "shading" (actually a misnomer here) is different from that of a matte object. Peaches are immediately distinguished (pure visually that is) from apples or tomatoes of roughly similar shape and color. (Figure 10.) They appear as "soft" to the eye, whereas apples look much "harder".

Likewise, the skin of young women is easily distinguished from surfaces of

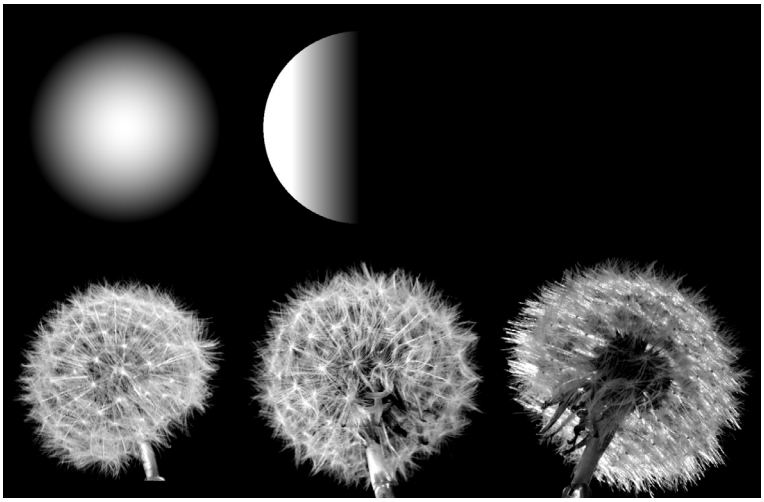

Figure 12: *At the bottom row we show three views of a dandelion pappus. Here the interior is (almost) empty and there is only a spherical shell of scatterers. Since you can look through single scattering apparently predominates. Left frontal illumination, at the center side illumination (phase angle* $90°$*), and on the right the a contre jour condition. Notice that the results in no way resemble those expected for a Lambertian sphere, as shown in the upper row (again, three views (!), the rightmost one being invisible because uniformly black).*

similar glossiness of materials of similar translucency. For instance, marble or chalcedony look "hard", whether a girl's skin looks "soft". (Figures 13 and 14.) We venture that the effect is due to asperity scattering, and that attempts to introduce translucency effects, specific varieties of gloss, etc., aimed at the rendering of skin are doomed to failure when the asperity lobe is not taken into account, even though its quantitative impact on the radiance of the scattered beams may be quite small.

Asperity scattering indeed typically has only a minor quantitative influence on the photometry, with the possible exception of the areas near the occluding boundary. Its qualitative effects can be considerable though.

For instance, it is generally acknowledged that computer graphics of the human complexion typically looks disappointingly like plastic. The characteristic weathered skin of middle aged or elder males (figure 13) can easily be simulated via a three–dimensional texture (*e.g.*, a bump map of tree bark–like relief). The smooth skin of children and young females (figures 13 and 14) is much harder to render. One (important) shortcoming of the BRDF approach has been identified as the translucency of young female skin. This

Figure 13: *Two portraits in profile with* a contre jour *illumination. The source is fully occluded by the heads. In the case of the elderly male face the white sideburns "catch the light" and appear as a bright halo. In the case of the young female essentially the same effect produces a bright contour although the hairs are two orders of magnitude shorter and would not normally be noticed at all. That this is a true case of asperity scattering (not an illuminated rim) is clear from the absence of scattering at the glabrous skin of the lips, where the bright halo is conspicuously interrupted.*

quality has often enough been noticed by poets and writers ("alabaster" or "milky" quality of skin) and it has recently been implemented in computer graphics[6]. Whereas this yields a highly noticeable improvement in realism, the skin still looks too "hard". This is understandable because the translucency blurs various surface features, shadow edges and so forth, thus lending a softer quality to the skin, but it leaves the occluding boundaries quite sharp. Indeed, in chalcedony cameos translucency is a dominant optical property, yet such artifacts look not soft at all but look hard as stone (as indeed they are of course).

A quality that has also often been noticed by poets and writers is the "peachy" or "velvety" quality of skin. This effect is quite different from translucency as it lends a soft look due to a softening and overall change of the nature of the occluding contour. This quality is doubtless due to asperity scattering. On close inspection young female faces are covered with almost invisible downy hairs that scatter in a similar way as peaches or velvet. (See

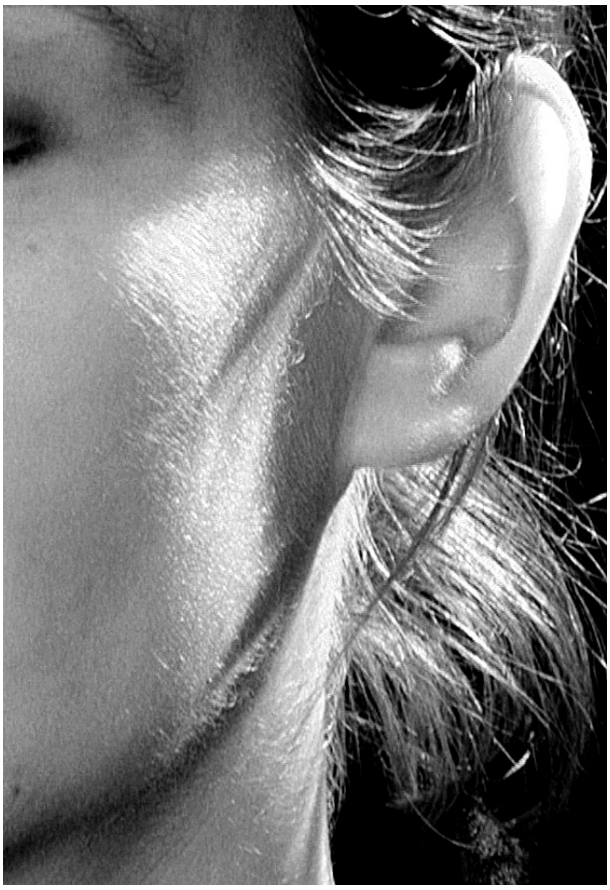

Figure 14: *Although one doesn't normally think of young women's cheeks as "hairy", they really are. Since the hair cover is sparse, and the hairs very thin and short, it is hardly noticeable in most circumstances except grazing illumination like here. The effects of asperity scattering are always present though, especially near the contours. Although one may not consciously notice, it makes the skin look "soft" and quite different from plastic (say) as in much of computer graphics rendering.*

figures 13 through 15.) The effect is quite noticeable in many photographs (we find that the effect is clear in more than half of the professional facial shots of models that are so plentiful on the internet) and can actually dominate in the case of *contre jour* illumination. Such effects have been used by painters who generally care very much about the precise nature of the occluding boundaries[5] . So far this has been neglected in computer graphics though.

In order to fully understand the importance of these effects it does not

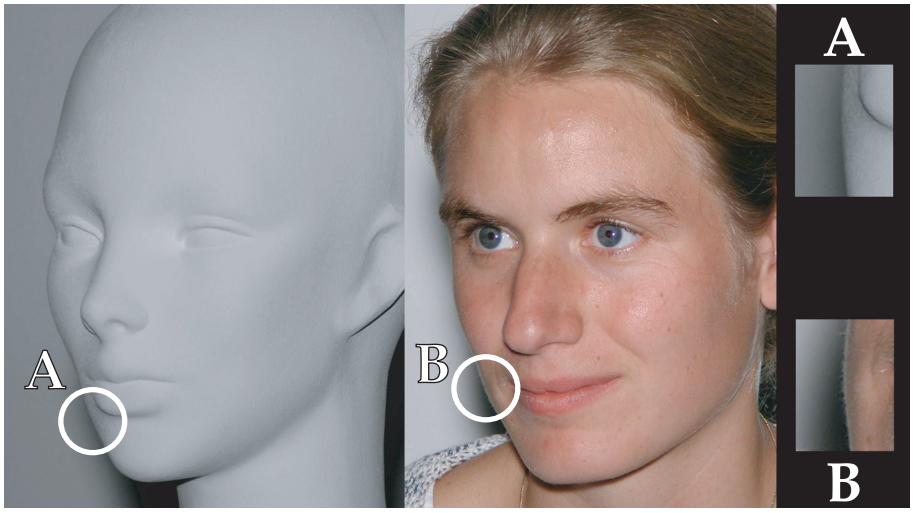

Figure 15: *A (roughly) Lambertian dummy head and a real human head in the identical light field. The illumination is by a collimated beam from about 5° vertically above the optical axis, as is indeed evident from the cast shadows below nose and chin. In the real face the effect of asperity scattering is evident from the light edges at the contours of the cheek (left), jaw and neck (right), upper lip and lower chin. (Compare the contours at A and B shown enlarged at the right.) That these are not due to either direct illumination or reflexes (from the light background for instance) is evident from the fact that such regions appear quite different (dark rimmed contours) in the dummy head. The effects of asperity scattering lend the real face a soft, "peachy" look.*

suffice to merely understand the physics of the optical interactions. It is equally important to have some understanding of the relevant (human) psychophysics. The human visual system encodes the retinal illuminance pattern at the peripheral nervous sites in terms of a multiscale account of local modulations of (log–)luminance in space and time[8]. The precise nature of the gradients at edges, etc., is of much greater impact than the absolute levels of uniform regions. This has been well documented[3, 12, 13] and is demonstrated by such well known psychophysical effects as the "Mach band" phenomenon and the "Cornsweet–Crane illusion". These effects are often used in artistic rendering. Artists know that the treatment of the contour has a decisive influence on what is perceived to "fill out" the contour[5]. For example the interiors of the black disks depicted in figure 16 look quite different, though printed with exactly the same density of ink. Since asperity scattering mainly affects the precise nature of the contours and the body shadow

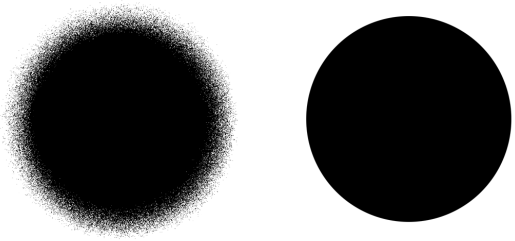

Figure 16: *A "hard" and a "soft" black disk on a white background. Notice that the interior of the soft disk looks "softer" (a fluffy or loose quality like blotting paper perhaps) and "less black" than that of the "hard disk" which looks blacker and "tighter" (like smooth plastic maybe). The difference in appearance is entirely due to the nature of the contour though, the interiors being actually identical.*

edges, its influence on the visual appearance largely exceeds what might be expected on the basis of a quantitative photometric analysis. In order for the rendering to look "convincing" it may be more important to get small effects near the critical edges at least qualitatively right, than to minimize the overall photometric error[5]. So far the relevant metrics are sadly lacking due to the fact that a psychophysics of realistic images is hardly available and one has to rely on artistic lore.

5 Discussion

We have outlined a simply theory of asperity scattering at the surfaces of solid objects. It is assumed that the scattering occurs in a thin layer covering the surface and that the scatterers are sparse, such that the single scattering approximation suffices. The typical asperity scattering lobe indeed relies on the predominance of single scattering, since multiple scattering would change the law of darkening dramatically. The exact nature of the scatterers is largely irrelevant. Examples include hairs standing on end or lying upon the surface, dust, fluff, localized sharp surface protrusions, and so forth. Examples abound in nature in plant surfaces (hairy leaves and stems), animal skin (fur, downy hairs) and many inorganic objects (due to dust for instance). They occur on many different scales, not just on the microscale. One may think of foliage or a wheat field from the distance for instance.

The generic effects of asperity scattering are bright haloes in contre jour illumination, light rimmed contours, light body shadow rims and effects of blur

and extension outside of the nominal "surface" and into the body shadow. All these effects make asperity scattering *very* different indeed from Lambertian or glossy objects. The photometric effects of asperity scattering tend to be small in the case of (nearly) normal incidence and viewing, in many cases much smaller than the photometric effects due to the other lobes (diffuse lobe, specular lobe, backscatter lobe). Thus asperity scattering can conveniently be treated as something "additional to" the standard shading effects.

We have shown that a very simple model accounts qualitatively, and—when the parameters are suitably adjusted—quantitatively for the observed effects. The free parameters are mainly the "turbidity" Δ/λ and the phase function $p(\cos\vartheta)$ (in most cases sufficiently characterized via one or two coefficients in a Legendre polynomials expansions). We have presented data on a sample of black velvet in the plane of incidence for which the model indeed leads to good quantitative understanding. We believe the model to be most useful as a rule of thumb and in qualitative modelling though. It is indeed quite intuitive, since the major effects are an inverse proportionality of the BDRF with the cosines of the illumination and viewing angles, and a direct proportionality with the phase function. This simple form makes that the effect of asperity scattering can be simply added to the standard graphics rendering pipelines.

We have argued that the effects of asperity scattering have a disproportionally (in terms of the photometric magnitudes) great effect on visual appearance. It seems likely that the spectacular failure to render human skin in a satisfactory manner has to do with the fact that the asperity scattering lobe is typically not taken into account. The rough surface (on a microscale) approximation accounts for the global shading and glossiness of skin. It yields the face relief (three dimensionality) and gives it the general look of plastic. Taking the natural translucency of flesh into account makes the rendering look much more convincing, but still yields a "hard" look, like alabaster or chalcedony perhaps. The asperity scattering due to downy, small hairs produces a more "peachy" feeling and yields a general feeling of softness. The effects of asperity scattering are indeed easily spotted in photographic portraits and accounts largely for the fact that photographs generally look more convincing than computer graphics renderings, even when the resolution doesn't suffice to render precise skin texture (pores, hairs).

Since asperity scattering is doubtless the prime cause of the peculiar "soft" look of smooth human skin, one wonders whether the cosmetics industry targets any products at this desirable property. Some skin products are clearly designed to influence the optics of skin, for instance, many fatty creams evidently aim at minimizing the effect of scattering by the superficial layer of dead, flaky skin cells, which produce a "dry" look (almost like

paper). These products minimize superficial scattering though optical immersion (matching the refractive index of the dead cells and the surrounding medium), thereby increasing the effects of the natural translucency. The effect of such products on asperity scattering remains to be studied. Products like face powders have the opposite effect. When a powder is applied sparingly and not rubbed into the skin (to be attached to the downy hairs would be ideal) asperity scattering is enhanced and a "soft" look results.

References

[1] Beckmann, P. and Spizzichino, A., *The Scattering of Electromagnetic Waves from Rough Surfaces*, Artech House, Norwood, Mass.: 1963.

[2] Chandrasekhar, S., *Radiative Transfer*, Dover, New York: 1960.

[3] Cornsweet, T., N., *Visual Perception*, Academic Press, New York: 1974.

[4] Hulst, H., C. van de, *Light Scattering by Small Particles*, John Wiley, New York: 1957.

[5] Jabobs, T., S., *Light for the Artist*, Watson–Guptill Publications, New York: 1988.

[6] Jensen, H., W., Marschner, S., R., Levoy, M. and Hanrahan, P., *A Practical Model for Subsurface Light Transport*, Proceedings of SIGGRAPH'2001, 2001.

[7] Koenderink, J. J, Doorn A., J. van, Dana, K., J, Nayar, S., K., *Bidirectional Reflection Distribution Function of thoroughly pitted surfaces*, International Journal of Computer Vision **31** (2/3), 129–144, 1999.

[8] Koenderink, J., J., Doorn, A., J. van, *Spatiotemporal Contrast Detection Threshold Surface is Bimodal*, Optics Letters **32**, 32-34, 1979.

[9] Kortüm, G., *Reflectance Spectroscopy: Principles, Methods, Applications*, Springer, Berlin: 1969.

[10] Lu, R., Koenderink J., J., Kappers, A., M., L., *Optical properties (bidirectional reflection distribution functions) of velvet*, Applied Optics **37** (25), 5974–5984, 1998.

[11] Lu, R., Koenderink J., J., Kappers, A., M., L., *Specularities on Surfaces with Tangential Hairs or Grooves*, Computer Vision and Image Understanding **78**, 320–335, 2000.

[12] Mach, E., *Die Analyse der Empfindungen und das Verhältnis des Physischen zum Psychischen*, Fischer, Jena: 1900.

[13] Metzger, W., *Gesetze des Sehens*, Waldemar Kramer, Frankfurt a. M.: 1975.

[14] Oren, M. and Nayar, S., K., *Generalization of the Lambertian Model and Implications for Machine Vision*, International Journal of Machine Vision **14**, 227–251, 1995.

[15] Lynch, D., K. and Livingston, W., *Color and Light in Nature*, Cambridge University Press, Cambridge: 1995.

5.0.1 Acknowledgements

We thank Michelle for modelling for figure 15.

Jan J. Koenderink graduated in Physics and Mathematics in 1967 at Utrecht University. He has been associate professor in Experimental Psychology at the Universiteit Groningen, then in 1974 returned to the Universiteit Utrecht where he presently holds a chair in the Department of Physics and Astronomy. He founded the Helmholtz Instituut in which multidisciplinary work in biology, medicine, physics and computer science is coordinated.

He has received an honorific degree (D.Sc.) in Medicine from the University of Leuven and is a member of the Royal Netherlands Academy of Arts and Sciences. He participates in the editorial boards of a number of scientific journals, scientific boards of international conferences and scientific institutes.

Research interests include cognitive science, ecological physics and machine intelligence.

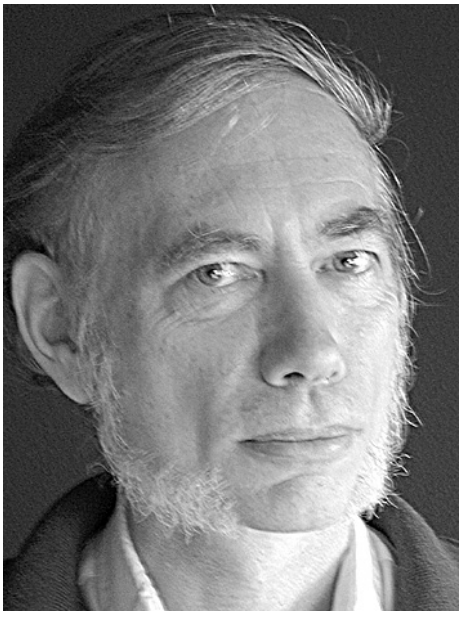

Sylvia C. Pont graduated in physics in 1993 at Amsterdam University, and received her PhD in 1997 at Utrecht University for a study into haptic shape perception. For two years she worked at the department of computer access technology of an institute for visually impaired people. In 1999 she returned to the Helmholtz Institute, Department Physics of Man, Utrecht University. Her research interests include optics of natural materials and psychophysics.